Available online at www.sciencedirect.com

SCIENCE DIRECT

Journal of the European Ceramic Society 26 (2006) 2475–2483

www.elsevier.com/locate/jeurceramsoc

Influence of the de-waxing atmosphere on the properties of AlN ceramics processed from aqueous media

S.M. Olhero [a], P. Miranzo [b], J.M.F. Ferreira [a,*]

[a] *Department of Ceramic and Glass Engineering, CICECO, University of Aveiro, 3810-193 Aveiro, Portugal*
[b] *Instituto de Cerámica y Vidrio, CSIC, Campus de Cantoblanco, 28049 Madrid, Spain*

Received 3 April 2005; received in revised form 2 June 2005; accepted 5 June 2005
Available online 22 July 2005

Abstract

The influence of binder burnout atmosphere (air or N_2) on surface chemistry of thermo-chemically treated AlN powders processed in aqueous media, and on the final properties of AlN ceramics was studied. The surface chemistry after de-waxing was accessed by scanning electron microscopy (SEM) and X-ray photoelectron spectroscopy (XPS). X-ray diffraction (XRD), SEM, high-resolution transmission electron microscopy (HR-TEM), were used to identify the phase assemblage and for microstructural analysis. The effects of the residual carbon and oxygen at the surface on the thermal conductivity and sintered density of AlN samples were investigated. The surface C/O ratios were observed to correlate with the sintering behaviour, the composition and distribution of secondary phases, and grain-boundary composition, as well as thermal conductivity of AlN samples. Thermal conductivities of about 140 W/mK were obtained for the aqueous processed AlN samples de-waxed in nitrogen atmosphere and sintered for 2 h at 1750 °C in the presence of 4 wt.% YF_3 + 2 wt.% CaF_2 as sintering additives.

Keywords: Sintering; Grain boundaries; Thermal conductivity; AlN; De-waxing

1. Introduction

High-performance advanced electronic packaging for high-density circuits and high-power transistors needs to have high thermal conductivity to dissipate the heat generated during functioning in order to have lower operational temperatures and improved reliability and performance. BeO and SiC are some of the most commonly used ceramic substrate materials for these applications. However, the high toxicity of BeO, the high dielectric constant of SiC and the high cost of both motivated the search for other alternative materials. In the last 10 years, AlN ceramics have been intensively studied for substrates applications due to the high thermal conductivity, non-toxicity and low dielectric constant among other properties.[1–3]

The thermal conductivity was found to depend on several factors, namely intrinsic and extrinsic. The intrinsic ones are material dependent such us the oxygen content (total and lattice dissolved), the microstructure, lattice defects among others, while the extrinsic ones are sintering conditions (atmosphere, furnace), sintering temperature, time and sintering additives. Hence, to achieve excellent properties of AlN, it is important to know how to optimize the extrinsic factors, which in turn influence the intrinsic ones.

One factor that promotes deleterious sintering is the presence of oxygen at the grain boundaries. In fact, along the sintering period, impurities such as oxygen are solid-dissolved in AlN crystal lattices or form a composite oxide, such as Al-O-N, which hinders the propagation of the thermal oscillations of the lattice. During firing, these impurities are incorporated into the AlN lattice by substitutional solution in the nitrogen site, creating aluminium vacancies, according to the following reaction (1):

$$Al_2O_3 \rightarrow 2Al_{Al} + [\cdot]_{Al} + 3O_N \qquad (1)$$

where $[\cdot]_{Al}$ denotes an aluminium vacancy.

---

[*] Corresponding author. Tel.: +351 234 370242; fax: +351 234 425300.
E-mail address: jmf@cv.ua.pt (J.M.F. Ferreira).

0955-2219/$ – see front matter © 2005 Elsevier Ltd. All rights reserved.
doi:10.1016/j.jeurceramsoc.2005.06.001

Mass and strain misfits caused by the vacant aluminium site increase the scattering cross section of phonons, which decreases the phonon mean free path, thereby lowering the thermal conductivity.

Taking into account the reasons exposed above, numerous efforts aimed at lowering the oxygen content within the AlN grains and grain boundaries to decrease the temperature of densification and consequently to reduce the costs of the AlN substrates.[4–8] The use of sintering aids has been the approach more extensively studied to enhance AlN densification and thermal conductivity.[9–18] If oxygen impurities in raw powders react with sintering aids to form stable alumina compounds at the grain boundaries of sintered AlN, oxygen impurities do not diffuse into AlN lattice and crystal defects are not produced. The thermodynamics and kinetics of oxygen removal by the sintering aids determine both the microstructure and the impurity level of AlN ceramics. Therefore, besides adequate selection of sintering aids, suitable sintering conditions are very important to prevent further increase in the oxygen content of the AlN powder.[19,20] A higher thermal conductivity is achieved if the grain boundaries are clean from sintering additives and the system is free of oxygen. This is accomplished by heat treatments that lead to liquid removal by evaporation or migration to concentrate at grain-boundary triple points.

All the sintering studies already reported have been directed to AlN samples processed in organic media.[3–17] The viability of using aqueous media for processing AlN at industrial level is strongly dependent on the final properties, namely thermal conductivity and mechanical properties. The achievement of comparable properties using water to disperse the powders (AlN + sintering aids) and aqueous suspensions to consolidate green bodies by colloidal shaping techniques or to granulate powders for dry pressing, will have enormous benefits in terms of health, economical and environmental impacts.

Further benefits will be obtained if the AlN ceramics processed from aqueous suspensions can be sintered at lower temperatures than those usually used (>1850 °C) to densify AlN ceramics processed in organic media without jeopardizing the final properties (high thermal conductivity, mechanical strength, etc.).

Aqueous processing of AlN needs a surface protection of the particles to avoid hydrolysis,[21,22] turning the system more complex. Therefore, transposing the findings of sintering studies using AlN samples prepared in organic media to samples processed in aqueous media is not straightforward. The coating layer composed of oxygen and phosphorous might turn the sintering behaviour ambiguous, and further studies are necessary. In fact, the surface layer used to protect the AlN particles could be a trouble for the sintering process, due to the rising amount of oxygen content at the surface of the AlN particles supplied by the protection layer.[21] Moreover, when binders and plasticizers are used as processing additives, such as in tape casting or powder granulation, it is necessary to remove these organic species prior to densification. Due to the easy oxidation of aluminium nitride in presence of oxygen and the residual carbon supplied by the organic species during burnout, the de-waxing atmosphere is a critical parameter.[23–27]

This work aims at studying the influence of de-waxing atmospheres on sintering and final properties of AlN processed in aqueous media. The water-based suspensions containing a binder and plasticizers were freeze granulated and the as obtained powders were used to consolidate AlN samples by dry pressing. The effects of the type of atmosphere used during burnout of binder and plasticizers on the surface chemistry of AlN and of different amounts of sintering additives (CaF_2 and YF_3), as well as their repercussions in the final properties of AlN samples sintered at a temperature as low as 1750 °C were studied.

2. Experimental procedure

2.1. Materials and processing

The aluminium nitride used in this work was supplied by Starck (Grade C, H.C. Starck, Berlin) and has an average particle size, $D_{50} \approx 0.33\ \mu m$, a specific surface area of $\approx 6\ m^2/g$, and an oxygen content of 2.5 wt.% O_2, according to the information given by the supplier. CaF_2 (Grade-325 mesh, 99.9%, Aldrich, Germany; $\rho = 3.18\ g/cm^3$) and YF_3 (99.9%, Aldrich, Germany, $\rho = 4.01\ g/cm^3$) were used as sintering aids.

An aqueous suspension containing 40 vol.% of mixtures of thermo-chemically treated AlN (AlN-T) powder with different weight proportions of CaF_2/YF_3 was prepared using the optimized dispersion conditions reported earlier[21] (1 wt.% of Duramax 3005, Rohm and Haas, Lauterbourg, France) and different amounts of binder (MDM2, ÁgoraMat, Aveiro, Portugal) and a polyvinyl alcohol-based plasticizer with an average molecular weight of 200 $g mol^{-1}$ (P200, ÁgoraMat, Aveiro, Portugal).

The compositions of the specimens and the respective sample codes are shown in Table 1.

The as-prepared suspensions were then granulated by freeze granulation (PowerPro freeze granulator LS-2, Gothenburg, Sweden) and the granules dried in a freeze-drying system (Labconco, LYPH Lock 4.5, Kansas City, USA) for several days. After completely dried, the granules were pressed in cylindrical pellets (20 mm diameter, 4 mm thickness), at a pressure of 90 MPa for 30 s, followed by isostatic pressing at 200 MPa.

Table 1
Sample codes and the respective compositions tested

Sample code	AlN-T	YF_3	CaF_2	Binder (wt.%)	Plasticizer (wt.%)
A	95	3	2	3	1.5
B	94	4	2	3	1.5
C	93	4	3	3	1.5

2.2. De-waxing and characterization of the AlN surface

In order to evaluate the effects of de-waxing atmospheres on oxidation extent of AlN particles, binder burnout was carried out in nitrogen atmosphere or in air at a heating rate of 5 °C/min from room temperature to 500 °C, 1 h holding time at this temperature, and free cooling down. Thermal analysis (SETARAM, Labsys, Caluire France) was performed in the two atmospheres (N_2 or air) to verify the thermal effects on weight loss and heat flow. X-ray photoelectron spectroscopy (XPS) analysis was used to access the surface chemistry of the AlN powder, namely to quantify the residual oxygen, carbon and phosphorous remaining at the surface of the AlN particles. The XPS analysis was performed using an ESCALAB 200A, VG Scientific (UK) with PISCES software for data acquisition and analysis. For analysis, an achromatic Al (Ka) X-ray source operating at 15 kV (300 W) was used, and the spectrometer, calibrated with reference to Ag 3d5/2 (368.27 eV), was operated in CAE mode with 20 eV pass energy. Data acquisition was performed with a pressure lower than 10−6 Pa. Spectra analysis was performed using peak fitting with Gaussian-Lorentzian peak shape and Shirley type background subtraction.

The fracture surfaces of the compacts after binder burnout in different atmospheres were observed by scanning electron microscopy (SEM, Hitachi S-4100, Tokyo, Japan).

2.3. Sintering and characterization of the AlN samples

After binder and plasticizers burnout, AlN samples were embedded in a 50 wt.% AlN and 50 wt.% BN powders mixture inside a graphite crucible and placed in a graphite furnace under nitrogen flow (40 kPa), and sintering was carried out according to the following schedule: 20 °C/min until 1250 °C, 10 °C/min from 1250 to 1650 °C, 1 h holding time at 1650 °C, 5°/min until 1750 °C with 2 h holding at this temperature.

Densities of samples were measured by Archimedes displacement method with diethyl-phthalate as the immersion medium. The percentage of densification (%TD) of the AlN species was calculated assuming a theoretical density of the aluminium nitride as 3.26 g/cm^3. The crystalline phases of the sintered specimens were identified using XRD (Rigaku, Tokyo, Japan) with Cu Kα radiation. Microstructure of fracture surfaces was observed by scanning electron microscopy (SEM, Hitachi S-4100, Tokyo, Japan).

The grain AlN boundaries were investigated by transmission electron microscopy (TEM, Hitachi, 9000 NA, Tokyo, Japan). The thermal diffusivity (α) was measured by the laser flash method using a commercial equipment (Thermaflash 2200, Holometrix, USA). Disk shaped samples of 12.7 mm of diameter and 1–2 mm of thickness were used for these measurements. The surfaces of the specimens were gold and graphite coated to avoid direct transmission of the laser pulse across the sample and to enhance absorption of the flash energy, respectively. Software based on Koski's method, which takes into account heat losses and finite pulse corrections, was used to relate the shape of the temperature-time curve with the diffusivity of the material. The value of thermal conductivity (K) of the tested materials was determined from Eq. (2):

$$K = \alpha C_p \rho \tag{2}$$

where C_p is the heat capacity [assumed to be the same as for pure dense aluminium nitride at 25 °C (≈0.8 J/g K)] and ρ the density of the material.

3. Results and discussion

3.1. Influence of de-waxing atmosphere on surface chemistry of AlN particles

The results of thermal analysis of the A-composition (see Table 1) carried out under oxidant (air) and inert (N_2) atmospheres are presented in Fig. 1 through the heat flow and weight loss curves. Under both atmospheres the weight loss presents successive steps, but the total weight loss is higher in the case of N_2 atmosphere. The differences become more evident for temperatures >400 °C where the weight loss due to organics removal in air is mitigated by some weight gain due to oxidation of AlN. Accordingly, the TG curve tends to a plateau, contrarily to the continuous decreasing trend observed in N_2. It is also worthwhile to note the shifting of TG curve to higher temperatures when carried out under inert atmosphere. The first steps of weight loss are attributed to the release of free and adsorbed water. The second steps of weight loss starting at ≈180 °C might be due to the degradation of lower molecular weight organic additive (plasticizer), while the third ones starting at ≈300 °C are attributed to decomposition of the binder.

As expected, there are big differences between DTA curves depending on the type of atmosphere, especially in the effects related to the burnout of organic additives. A strong exothermic peak is observed in air, while the opposite effect is observed in inert atmosphere. It can be predicted that the exothermic removal of the organics in ambient atmosphere

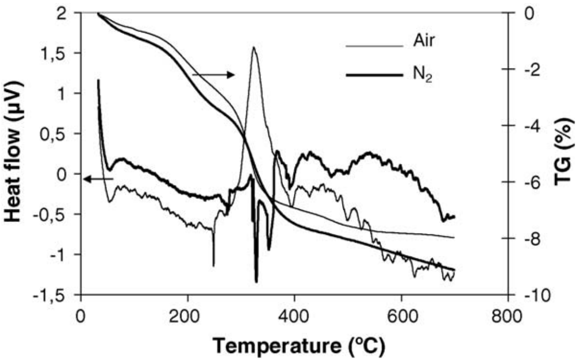

Fig. 1. DTA/TG (heat flow/weight loss) curves of composition A under different atmospheres: (Air and Nitrogen).

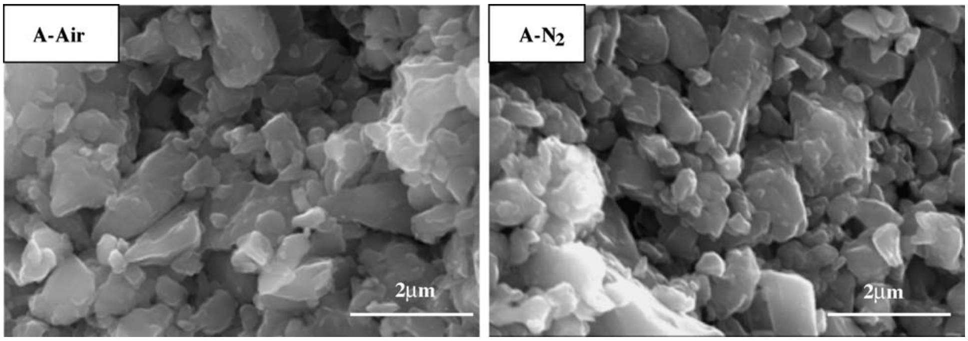

Fig. 2. Fracture surfaces of A-samples after de-waxing under different atmospheres: (a) Air; (b) Nitrogen.

can lead to localized heating in a thick body and defects like hot spots delamination or anisotropic shrinkage. The most part of processing additives has been burnout at ≈350 °C (air) and at ≈375 °C (N_2). Based on these results, de-waxing experiments aiming at evaluating the influence of the atmosphere on surface chemistry were conducted up to 500 °C.

The effect of ambient atmosphere on oxidation of AlN has been evaluated by microstructural SEM observations and reported in earlier works by other authors.[19,28–31] The studies have been carried out at temperatures in the range of 1000–1400 °C for relatively long time periods (20–100 h). Generally, the authors found a porous thin film structure at the interface where oxidation took place composed essentially by Al_2O_3 or $5Al_2O_3·3Y_2O_3$. This surface oxide layer was severely cracked because of the thermal expansion mismatch between the oxide layer and the substrate, decreasing the flexural strength of the material.

In the present work, attempts were made to evaluate possible effects of de-waxing atmosphere on the SEM microstructures of fracture surfaces of all AlN sample compositions. Fig. 2 refers to the A-composition (see Table 1) and reveals that there is no detectable difference between the two atmospheres. Similar observations were made for the other compositions. These similar SEM results can be explained by the lower temperature (500 °C) and the shorter time (1 h) used in the present work and the low sensitivity of SEM to detect such small effects.

Contrarily, the XPS technique revealed to be suitable for accessing the differences in surface chemical compositions of AlN particles after de-waxing under the different atmospheres. Table 2 presents the amounts of carbon, oxygen, phosphorous, aluminium and nitrogen measured for the different AlN powders, as-received (AlN), after thermochemical treatment (AlN-T), and for the samples A, B and C after de-waxing under different atmospheres (air or N_2). The ratios between the different elements, O/Al, N/Al and C/Al are also shown.

Comparing the results for AlN and AlN-T powders, it is clear that there was an important surface enrichment in oxygen (≈9–10 wt.%) and P (≈8 wt.%) elements attributed to the phosphate species of the protective layer against hydrolysis, and a concomitant depletion of N and Al elements, confirming the results of an earlier report.[21] The decrease of the amount of aluminium at the surface of the AlN-T might also be partially due to a possible reaction between the oxygen and the aluminium to form aluminium oxide and oxynitride.[32,33]

Comparing the results for AlN-T and the compositions A, B and C after de-waxing in air atmosphere, it can be concluded that the surface of AlN particles becomes about 1 wt.% riched in oxygen after the burnout step. On the other hand, de-waxing in N_2 atmosphere results in significant decrease of the amount of oxygen (≈4 wt.%) and a concomitant increase in the carbon content (≈8–9 wt.%). The analysis of the atomic ratios between the different elements reveals that O/Al ranges

Table 2
Comparison of surface composition measured by XPS of the as received AlN powder with those of AlN-T powders before and after de-waxing under different atmospheres (air or nitrogen)

Elements	Content (at.%)							
	AlN	AlN-T	Sample A		Sample B		Sample C	
			Air	N_2	Air	N_2	Air	N_2
C (1s)	12.61	12.91	13.79	20.96	12.81	21.63	13.96	21.68
N (1s)	16.99	9.35	6.05	6.21	6.19	6.54	6.14	6.38
O (1s)	35.75	44.97	45.86	40.84	45.91	40.84	45.98	40.68
Al (2p)	34.65	24.97	26.06	23.79	26.52	23.44	25.73	23.08
P (2p)	–	7.80	8.24	8.20	8.58	7.55	8.18	8.19
O/Al	–	–	1.76	1.72	1.73	1.74	1.79	1.76
N/Al	–	–	0.23	0.26	0.23	0.28	0.24	0.28
C/Al	–	–	0.53	0.88	0.48	0.92	0.54	0.94

from 1.73 to 1.79 for the samples de-waxed in air, and between 1.72 and 1.76 for the specimens de-waxed in N_2. On the other hand, the N/Al is 0.23–0.24 for the first set and 0.26–0.28 for the latter one. However, differences in the C/Al atomic ratio are the largest: 0.48–0.54 in air, and 0.88–0.94 in N_2. These results are in good agreement with the findings of other authors.[24] Therefore, the binder burnout process left a significant amount of residual carbon on the AlN surface, which is larger in the case of the samples heat treated in nitrogen. By analysing the C1s peak, Yan et al.[24] concluded that the first layer of carbon is bound to oxygen atoms at the AlN surface while additional carbon is bound to carbon itself, forming amorphous graphitoid carbon clusters which covered the powder surface uniformly.

In spite of carbon increasing after binder burnout, oxygen content seems to be the most abundant element at the surface of all AlN powders. Therefore, the use of proper amounts of sintering aids is of crucial importance to help releasing the excess of oxygen.

Recently, Robinson and coworkers found that oxygen distribution was not continuous along thickness direction of the oxidized AlN.[29,30] They suggested that additives enhancing densification may be critically important to the oxidation kinetics of AlN polycrystals and the oxidized structure as well. Wenjea Tseng et al.[28] also supported this proposition by showing that the additive chemistry and the doping level both play crucial roles in determining the oxidation behaviour of fully sintered AlN.

In the present work, the used of different amounts and proportions of sintering additives did not affect the surface chemistry of AlN particles after de-waxing, but influenced the thermal properties after sintering, as will be discussed below.

3.2. *Influence of de-waxing atmosphere on the properties of sintered AlN ceramics*

The results of density and thermal conductivity of the different AlN-based compositions after de-waxing (in air or nitrogen) and sintering at 1750 °C for 2 h are reported in Table 3. Considering that the standard deviation of sintered density is ±0.1%, one can conclude that full densification was obtained for all the compositions tested, independently of the de-waxing atmosphere used. The values of thermal conductivity are also reported in Table 3, with a standard deviation of ±5%. Since all samples reached full density, the observed differences in thermal conductivity cannot be attributed to the densification degree. The nature and concentration of sintering aids and the de-waxing atmosphere are the most relevant factors determining thermal conductivity, which in turn depends on the microstructural features and on the crystalline phases formed. Besides A, B, and C specimens have similar thermal conductivity values considering the accuracy of the laser flash technique, a slight increase with increasing

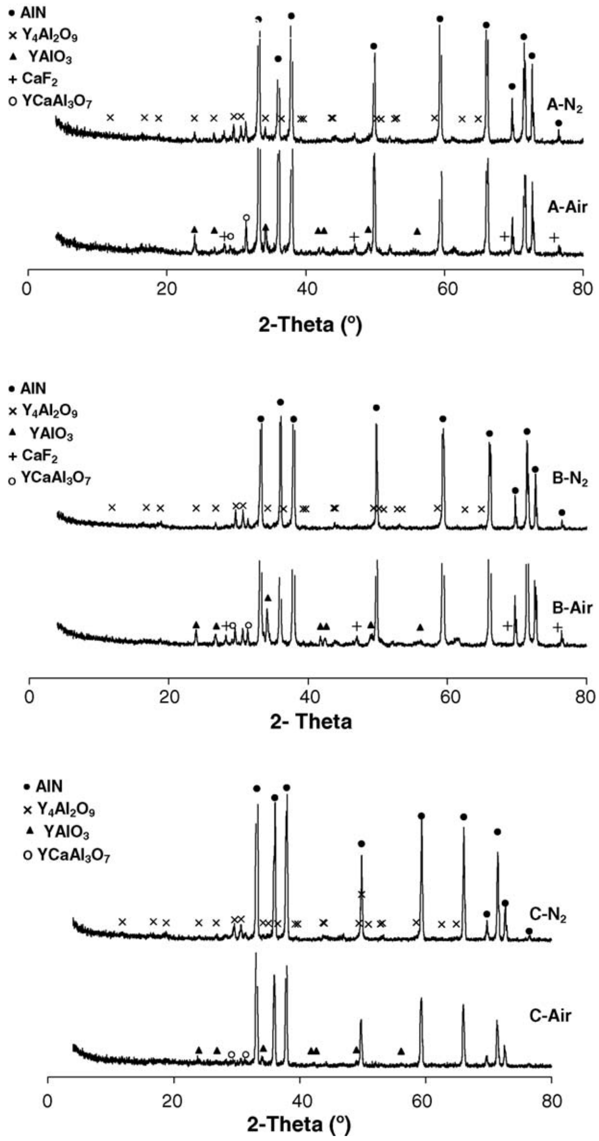

Fig. 3. X-ray powder diffraction patterns of A, B and C compositions after de-waxing in air or nitrogen.

Table 3
Density and thermal conductivity values of the sintered specimens

Samples	Measured sintered densities (g/cm^3)		Thermal conductivity (W/m K)[a]	
	De-waxing in air	De-waxing in N_2	De-waxing in air	De-waxing in N_2
A	3.261 ± 0.005	3.255 ± 0.008	111	125
B	3.258 ± 0.003	3.258 ± 0.002	111	136
C	3.251 ± 0.005	3.257 ± 0.007	119	136

[a] The standard deviation values for thermal conductivity measurements were ±5%.

the amount of additives is apparent. On the other hand, significant differences (increases of 22%) in thermal conductivity are observed when comparing the data of samples sintered in air and in nitrogen. Differences in oxygen content detected by XPS are only at a thin surface layer (a few nanometers) of the AlN grains and therefore they do not affect to the mean phonon free path and cannot explain the observed differences in thermal conductivity. These differences might be related to the secondary intergranular crystalline phases.

Fig. 3 shows that the secondary crystalline phases formed during sintering are dependent on de-waxing atmosphere, and on the total amount and ratio of sintering additives. As expected, the major crystalline phase was identified as AlN, for all compositions tested. However, the intensity and resolution of AlN peaks were enhanced when de-waxing was in nitrogen atmosphere and with increasing the total amount of sintering aids to 7 wt.%. Additional peaks were registered which could be consistently indexed as corresponding

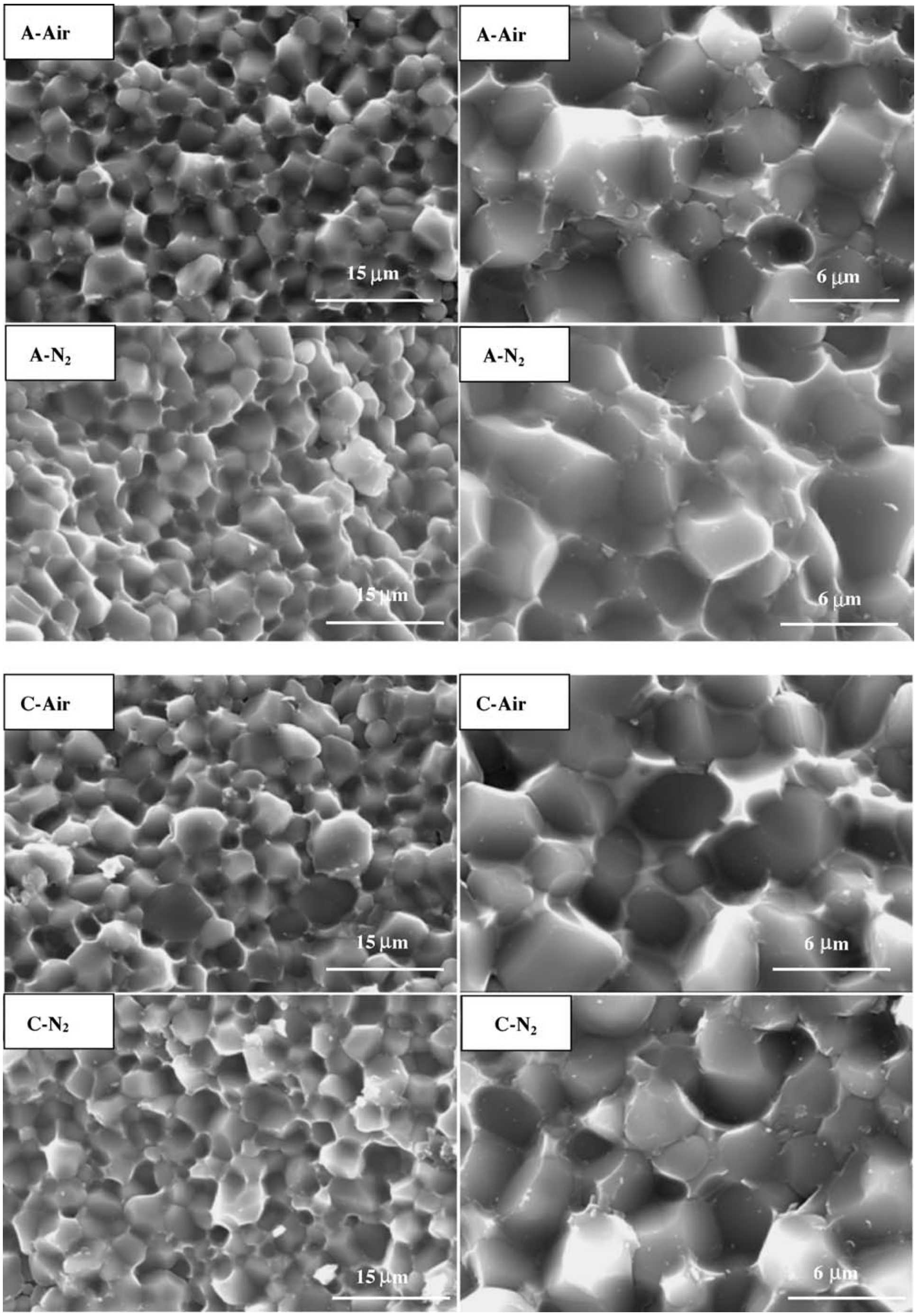

Fig. 4. Microstructures of fracture surfaces of samples A and C sintered at 1750 for 2 h after de-waxing in air or nitrogen.

to yttrium aluminium monoclinic (YAM-$Y_4Al_2O_9$) when nitrogen atmosphere was used, while yttrium aluminium perovskite (YAP-$YAlO_3$) or $YCaAl_3O_7$ were formed when de-waxing was made in air. The origin of these secondary crystalline phases in the sintered samples is postulated to be as follows. The surface of AlN treated powder contains significant amounts of oxygen and phosphorous coming from the protective layer against hydrolysis. XPS analysis revealed that the phosphorous element still present at the surface of AlN powders after de-waxing at 500 °C (Table 2) could no more be detected after heat treating the samples at temperatures ≥1400 °C (temperature of liquids). This means that P element volatilizes upon heating up to 1400 °C. The formation of liquid phase is expected to occur at ≈1400 °C, according to the phase diagram.[34] The oxygen remaining at particles' surface reacts with the sintering additives (YF_3 and CaF_2) to form a low melting point eutectic phase. This liquid phase assists the densification process and gives rise to crystalline phases, such as YAM or YAP, either precipitated during sintering or on solidification. It is worthwhile to note that the yttrium-richer second phases were formed when the de-waxing was made in nitrogen atmosphere. Therefore, a correlation between the C/O atomic ratio at the AlN powder surface and the Al/Y/Ca in the second phase of the sintered material can be found. In fact, secondary intergranular phases became yttrium-richer ($Y_4Al_2O_9$) as surface C/O ratio increases, consequently enhancing the thermal conductivity (Table 3). The change of the secondary intergranular phases from aluminium-rich to yttrium-rich can be understood based on carbon de-oxidation during sintering, which removes oxygen impurities from the grain boundaries according to the following chemical reaction:

$$Al_2O_3 + 3C + N_2 \rightarrow 2\,AlN + 3CO \qquad (3)$$

The above results are in good agreement with those reported by other authors who defended that when $Y_4Al_2O_9$ is formed in AlN-Y_2O_3 ceramics instead of $Y_3Al_5O_{12}$ or $YAlO_3$, the highest thermal conductivity can be achieved.[10]

The distribution of the secondary phases in the samples, which may contribute to the increase in thermal conductivity, was also found to be dependent on C/O ratio.[24] The effect of

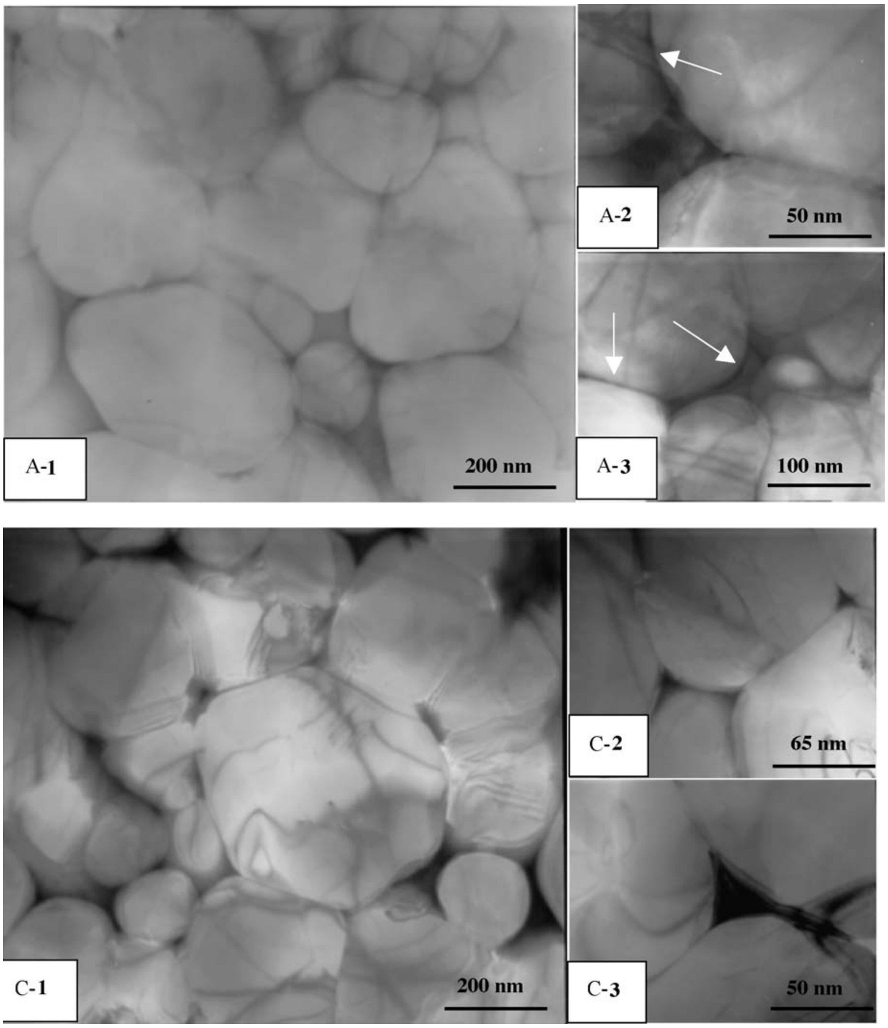

Fig. 5. TEM images of samples A and C sintered at 1750 for 2 h after de-waxing in Air.

de-waxing atmosphere on microstructural features of fracture surfaces of sintered samples A and C (see Table 1) can be observed in Fig. 4. A similar microstructure was observed for sample B (not shown).

All the microstructures confirm the high degrees of densification measured and show well-developed polyhedral grains. Sharper grain-boundary edges in pictures A-N_2 and C-N_2 indicate smaller amounts of grain-boundary phases and decreased wetting ability that led to a preferential segregation of liquid phase at the triple points. However, the influence of carbon on grain size seems to be less evident in the present work in comparison to the findings of Rang-Rong Lee,[35] who reported a decrease of grain size and an increase of thermal conductivity by adding about 0.5 wt.% carbon to AlN samples. According to these authors, carbon provides a temporary atmosphere suitable for reducing the level and the amount of alumina available to react with the sintering aids at the surface of the AlN powders. Besides decreasing grain size, these effects will enhance the formation of yttrium-rich secondary phases and concomitantly reduce the aluminium-rich ones at grain boundaries, as well as aluminium vacancies in the AlN grains, improving thermal conductivity.

TEM analysis was used to better characterise the inter-granular phases. Figs. 5 and 6 show the TEM images of the sintered samples A and C de-waxed in air and in nitrogen, respectively. It can be seen that AlN grains are separated by grain-boundary films, the thickness of which depend on the type of de-waxing atmosphere. The results of EDS analysis of the inter-granular films (not shown) revealed that they consist of different proportions of Y, O, Al and N, being more yttrium-rich when de-waxing was in N_2. In samples A and C de-waxed in air, the inter-granular films extend along the whole grain boundaries showing good wetting properties. The presence of these grain boundaries films disrupts the connections between grains and consequently decreases the thermal conductivity. Contrarily, the inter-granular film in sample A and C de-waxed in N_2 atmosphere is thinner and the secondary phases are apparently less abundant and appear preferentially located at the triple points. These differences can be related to the surface composition of the AlN grains. The higher C/Al atomic ratios (see Table 2) of the samples sintered in N_2 atmosphere will decrease the ratio between the grain-boundary energy (γ_{ss}) and the solid–liquid interfacial energy (γ_{sl}), γ_{ss}/γ_{sl}, leading to the isolated structure of the second phase observed in these specimens and increasing the thermal conductivity.

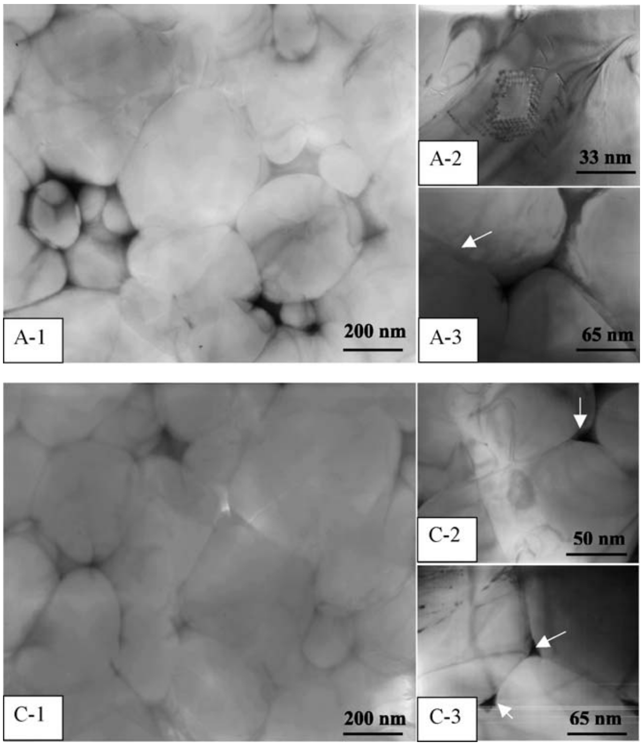

Fig. 6. TEM images of samples A and C sintered at 1750 for 2 h after de-waxing in Nitrogen.

Table 3 shows that increasing the total amount of sintering additives and the YF_3/CaF_2 ratio enhances thermal conductivity. It is suggested that the formation of Y-richer secondary phases de-wets the grain boundaries and segregates the inter-granular phases preferentially to the triple points leading to a more effective AlN–AlN grain-boundary contact.[18]

The TEM images also reveal some dislocations in AlN grains. The dislocation density is much lower in the samples that have been de-waxed in N_2. The image A-2 in Fig. 6 shows a particular and much localised case of high dislocations density found in an AlN grain of the A-sample de-waxed in N_2. However, the samples de-waxed in air display an overall high dislocations density, forming a kind of network. The presence of defects, such as dislocations is harmful to thermal conductivity of AlN by acting as oxygen-gathering defects that remove oxygen from large parts of the bulk grains or grain boundaries.

4. Conclusions

Practically full dense AlN ceramics having thermal conductivities varying from 110 to 140 W/m K have been successfully produced from granulated powders processed in aqueous media. De-waxing atmospheres, sintering aids and firing conditions were identified as key processing parameters in controlling density and thermal conductivity. The burnout of organic additives in N_2 atmosphere left a significant amount of residual carbon at the AlN powder surface that partially removes the excess oxygen. The reaction between the remaining excess oxygen and the sintering additives (CaF_2 and YF_3) leads to the formation of yttrium-richer ($Y_4Al_2O_9$) secondary phases preferentially located at the triple points that enhance thermal conductivity. Contrarily, de-waxing in air favours the formation of more abundant alumina-richer yttrium aluminates that better wet the AlN grains and spread along the whole grain boundaries, increasing the density of structural defects, such as dislocations, therefore decreasing thermal conductivity.

Acknowledgements

The first author wishes to thanks to *Fundação para a Ciência e Tecnologia of Portugal* for the financial support under the grant SFRH/BD/8754/2002. Thanks are also due to Project *PRAI-Centro* for the financial support. The second author is in debt to Mcyt (Ministery of Science and Technology, Spain), project MAT 2003-06147-C04-01.

References

1. Raether, F., Klimera, A., Thimm, A., Ruska, J., Mussler, B. and Brunner, D., High strength and high thermal conductivity of aluminium nitride ceramics by microstructural design. In *Symposium K5 multifunctional ceramics*, 2001.
2. Jackson, T., Barrett, Virkar, A. V., More, K. L., Dinwiddie, R. B. and Cutler, R. A., High-thermal-conductivity aluminium nitride ceramics: the effect of thermodynamic, kinetic and microstructural factors. *J. Am. Ceram. Soc.*, 1997, **80**(6), 1421–1435.
3. Collange, A., Grosseau, P., Guilhot, B., Disson, J. P. and Joubert, P., Thermal conductivity of compacted AlN samples. *J. Europ. Ceram. Soc.*, 1997, **17**, 1897–1900.
4. Qiao, L., Heping, Z., Xue, H. and Wang, S., Effect of Y_2O_3 on low temperature sintering and thermal conductivity of AlN ceramics. *J. Europ. Ceram. Soc.*, 2003, **23**, 61–67.
5. Streicher, E., Chartier, T., Boch, P., Denanot, M. F. and Rabier, J., Densification and thermal conductivity of low-sintering-temperature AlN materials. *J. Europ. Ceram. Soc.*, 1990, **6**, 23–29.
6. Liu, Y., Zhou, H., Qiao, L. and Wu, Y., Low-temperature sintering of aluminium nitride with YF_3-CaF_2 binary additive. *J. Mater. Sci. Lett.*, 1999, **18**, 703–704.
7. Jarrige, J., Bouzouita, K., Doradoux, C. and Billy, M., A new method for fabrication of dense aluminium nitride bodies at temperatures as low as 1600 °C. *J. Europ. Ceram. Soc.*, 1993, **12**, 279–285.
8. Thomas, B. T. and Nicholson, P. S., Effect of additives on the pressureless sintering of aluminium nitride between 1500 and 1800 °C. *J. Am. Ceram. Soc.*, 1989, **72**(8), 1488–1491.
9. Khan, A. A. and Labbe, J. C., Aluminium nitride-molybdenum ceramic matrix composites. influence of molybdenum addition on electrical, mechanical and thermal properties. *J. Europ. Ceram. Soc.*, 1997, **17**(15/16), 1885–1890.
10. Virkar, A. V., Barret, J. T. and Cutler, R. A., Thermodynamic and kinetic effects of oxygen removal on the thermal conductivity of aluminium nitride. *J. Am. Ceram. Soc.*, 1989, **72**(11), 2031–2042.
11. Qiao, L., Zhou, H. and Fu, R., Thermal conductivity of AlN ceramics sintered with CaF_2 and YF_3. *Ceram. Int.*, 2003, **29**, 893–896.
12. Yu, Y.-D., Hundere, A. M., Hoier, R., Dunin-Borkowski, E. and Einarsrud, M. A., Microstructural characterization and microstructural effects on the thermal conductivity of AlN (Y_2O_3) ceramics. *J. Europ. Ceram. Soc.*, 2002, **22**, 247–252.
13. Hundere, A. M. and Einarsrud, M. A., Microstructural development in AlN (YF_3) ceramics". *J. Europ. Ceram. Soc.*, 1997, **17**, 873–878.
14. Terao, R., Tatami, J., Meguro, T. and Komeya, K., Fracture behaviour of AlN ceramics with rare earth oxides. *J. Europ. Ceram. Soc.*, 2002, **22**, 1051–1059.
15. Boey, F., Cao, L., Khor, K. A. and Tok, A., Phase reaction and sintering behaviour of a Al_2O_3-20 wt.%AlN-5 wt.% Y_2O_3 system. *Acta Materialia*, 2001, **49**, 3117–3127.
16. Buhr, H. and Muller, G., Microstructure and thermal conductivity of AlN (Y_2O_3) ceramics sintered in different atmospheres. *J. Europ. Ceram. Soc.*, 1993, **12**, 271–277.
17. Watari, K., Hae, J. H., Toriyama, M. and Kanzaki, S., Effective sintering aids for low-temperature sintering of AlN ceramics. *J. Mater. Res.*, 1999, **14**(4), 1409–1417.
18. Hundere, A. M. and Einarsrud, M. A., Effects of reduction of the Al-Y-O containing secondary phases during sintering of AlN with YF_3 additions. *J. Europ. Ceram. Soc.*, 1996, **16**, 899–906.
19. Lavrenko, V. A. and Alexeev, A. F., Oxidation of sintered aluminium nitride. *Ceram. Int.*, 1983, **9**(3), 80–82.
20. Wang, M. C., Yang, C. C. and Wu, N. C., Grain growth and electric properties of liquid phase sintered AlN. *Mater. Eng.*, 2003, **A343**, 97–106.
21. Olhero, S. M., Novak, S., Krnel, K., Kosmac, T. and Ferreira, J. M. F., Thermo-chemical Surface Treatment of AlN Powder Towards Aqueous Processing of AlN Ceramics. *J. Mater. Res.*, 2004, **19**(3), 746–751.
22. Oliveira, M., Olhero, S., Rocha, J. and Ferreira, J. M. F., Controlling hydrolysis and dispersing AlN Powders in aqueous media. *J. Colloid Interface Sci.*, 2003, **261**, 456–463.
23. Gorzawski, G., Sternitzke, M., Muller, W. F., Berger, A. and Muller, G., Oxygen enrichment at inversion domain boundaries in aluminium nitride-influence on thermal conductivity. *J. Europ. Ceram. Soc.*, 1995, **15**, 95–99.
24. Yan, H. W., Cannon, R. and Shanefield, D. J., Evolution of carbon during binder burnout and sintering of tape-cast aluminium nitride. *J. Am. Ceram. Soc.*, 1993, **76**(1), 166–172.
25. Nakano, H., Watari, K. and Urabe, K., Grain-boundary phase in AlN ceramics fired under reducing N_2 atmosphere with carbon. *J. Europ. Ceram. Soc.*, 2003, **23**, 1761–1768.
26. Boch, P., Glandus, J. C., Jarrige, J., Lecompte, J. P. and Mexmain, J., Sintering Oxidation and mechanical properties of hot pressed aluminium nitride. *Ceram. Int.*, 1982, **8**(1), 34–40.
27. Ichinose, N., Effect of carbon-reducing atmosphere on the properties of aluminium nitride (AlN). *Mater. Chem. Phys.*, 1995, **42**, 176–180.
28. Wenjea, J., Tseng and Tsai, C. J., Microporous layer structure in oxidized aluminium nitride polycrystals. *J. Mater. Process. Technol.*, 2004, **146**, 289–293.
29. Robinson, D. and Dieckmann, R., Oxidation of aluminium nitride substrates. *J. Mater. Sci.*, 1994, **29**, 1949–1957.
30. Robinson, D. A., Yin, G. and Dieckmann, R., Oxide film formation on aluminium nitride substrates covered with thin aluminium layers. *J. Mater. Sci.*, 1994, **29**, 2389–2394.
31. Hyoun-Ee, K. and Moorhead, A. J., Oxidation behaviour and flexural strength of aluminium nitride exposed to air at elevated temperatures. *J. Am. Ceram. Soc.*, 1994, **77**(4), 1037–1041.
32. Osborne, E. W. and Norton, M. G., Oxidation of aluminium nitride. *J. Mat. Sci.*, 1998, **33**, 3859–3865.
33. Bellosi, A., Landi, E. and Tampieri, A., Oxidation behaviour of aluminium nitride. *J. Mater. Res.*, 1993, **8**(3), 565.
34. Roth, R. S., Negas, T. and Lawrence, P. C., In *Phase diagrams for Ceramists, Vol. 5*, ed. G. Smith. American Ceramic Society, 1983. pp. 97 (figures) and 5793.
35. Ran-Rong Lee, Development of high thermal conductivity aluminium nitride. *J. Am. Ceram. Soc.*, 1991, **74**(9), 2242–2249.